Doping radius effects on an erbium-doped fiber amplifier

Md. Ziaul Amin[1,*], Khurram Karim Qureshi[2,], and Md. Mahbub Hossain[3,***]**

[1]*MQ Photonics, School of Engineering, Macquarie University, New South Wales 2109, Australia*
[2]*Department of Electrical Engineering, King Fahd University of Petroleum and Minerals, Dhahran 31261, Saudi Arabia*
[3]*Electronics and Communication Engineering Discipline, Khulna University, Khulna 9208, Bangladesh*
**Corresponding author: md-ziaul.amin1@students.mq.edu.au; **corresponding author: kqureshi@kfupm.edu.sa; ***corresponding author: mahbub.eceku@yahoo.com*

Received August 23, 2018; accepted November 12, 2018; posted online December 20, 2018

In an erbium-doped fiber amplifier (EDFA), erbium ions act as a three-level system. Therefore, much higher pump energy is required to achieve the population inversion in an erbium-doped fiber (EDF). This higher pump energy requirement complicates the efficient design of an EDFA. However, efficient use of the pump power can improve the EDFA performance. The improved performance of an EDFA can be obtained by reducing the doping radius of the EDF. A smaller doping radius increases pump–dopant interactions and subsequently increases the pump–photon conversion efficiency. Decreasing the doping radius allows a larger proportion of dopant ions, which are concentrated near the core, to interact with the highest pump intensity. However, decreasing the doping radius beyond a certain limit will bring the dopant ions much closer and introduce detrimental ion–ion interaction effects. In this Letter, we show that an optimal doping radius in an EDF can provide the best gain performance. Moreover, we have simulated the well-known numerical aperture effects on EDFA gain performance to support our claim.

OCIS codes: 060.2310, 060.2410, 140.4480.
doi: 10.3788/COL201917.010602.

Long-distance point-to-point optical communication links and optical networks are limited by the various fiber losses. Therefore, compensation of the fiber losses can help in realizing long-distance fiber optic communication systems. The losses can be compensated by introducing amplifiers in the optical link. Initially, only semiconductor laser amplifiers were used to amplify the optical signal, which are incompatible with optical fiber systems[1]. Moreover, optical–electrical and electrical–optical signal conversion is required in conventional semiconductor laser amplifiers, which makes the system more complex and increases the installation cost. These problems have been solved by introducing optical amplifiers, which can amplify the optical signal directly in the optical domain and are compatible with telecommunication fibers. The first fiber optic amplifier using erbium-doped fiber (EDF) was reported by Mears *et al.* in 1987[2]. This doped fiber amplifier can be operated in the low-loss window of the silica fiber and provides other advantages like high gain, high saturation output power, polarization independent gain, no cross-talk, low noise figure, and low insertion loss[3,4]. Moreover, this amplifier is the key component of wavelength division multiplexer (WDM) systems. Before this type of amplifier was available, one had to split all of the data channels and detect and amplify them electronically. Then, the amplified electrical signals were again converted to the optical domain and combined for transmission. Therefore, introduction of fiber amplifiers has reduced the complexity enormously and increased the reliability[5,6]. For meeting the demands of the many potential applications, further performance enhancement of optical amplifiers is needed.

Various parameters, such as pumping wavelength, numerical aperture (NA), cutoff wavelength, host glass, dopant concentration, dopant distribution, and amplifier configuration determine fiber amplifier performance. Two pump wavelengths, 980 nm and 1480 nm, which are free from excited-state absorption (ESA), are normally used for efficient EDF amplifier (EDFA) performance. For achieving the maximum performance from the EDFA, it is important to maximize the pump intensity in the dopant region to invert a sufficient number of ions. This can be achieved by using high NA fibers. Increasing the fiber NA results in a pump spot size decrease, and consequently, a pump intensity increase inside the fiber core[3,7,8]. A smaller cutoff wavelength in a single mode fiber is also advantageous for increasing the pump intensity.

Moreover, the pump conversion efficiency in an EDFA can be increased by reducing the doping radius of an EDF. This phenomenon has been reported by Armitage to theoretically enhance the EDFA performance[9]. A smaller doping radius removes ions from those sections of the EDF core where pump absorption is quite small. Therefore, pump absorption can be enhanced by increasing the interaction between the active ions and the pump signal. Due to the Gaussian nature of the fundamental pumping mode, the pump intensity at the center of the core is the highest. This characteristic of the pump signal increases the interaction of the pump signal and the dopant

ions, which subsequently improves the pump absorption in an EDF. As the pump absorption is increased, which excites more ions to upper energy states, the EDFA gain performance is enhanced. Another research group led by Ainslie fabricated an EDF using a Al_2O_3–P_2O_5–SiO_2 glass host, where dopant ions were confined to the center of the core, and reported improved EDFA performance[10]. Ohashi also showed that decreasing the doping radius theoretically increases the signal gain[11].

However, concentrating the dopant ions near the center of the core will reduce the distance between the dopant ions and increase the detrimental clustering effects. Due to these clustering effects, energy between fractions of clustered ions is transferred very rapidly and reduces the excited-state population, which is well-known as pair induced quenching (PIQ). Myslinski *et al.* presented a theoretical and experimental study of EDFA performance degradation due to PIQ[12]. Introducing inhomogeneous cooperative upconversion, the gain degradation of an EDFA was modeled by another research group led by Masuda and his fellow authors[13]. They used their model to explain an experimental result of low gain in an EDFA with high dopant concentration. Considering the homogeneous and inhomogeneous upconversion, EDFA performance degradation due to Er^{3+}–Er^{3+} interaction was simulated in Ref. [14]. Recently, our group investigated the detrimental clustering effects on the lasing performance of an EDF laser (EDFL)[15].

In this Letter, we have simulated the EDFA performance by varying the doping radius of erbium ions and found that there is an optimal doping radius, which can provide the best EDFA gain performance. For the optimal doping radius, the interaction between pumping energy and dopant ions is at a maximum, and ion–ion interaction is at a reasonable limit. This phenomenon of enhanced pumping efficiency can be explained by dividing the core area into two regions: absorption and amplification regions, as explained in the following section.

At a 980 nm pumping wavelength, Er^{3+} works as a three-level system, as shown in Fig. 1. Pump energy excites the Er^{3+} and lifts it from the ground energy level ($^4I_{15/2}$) to the pump level ($^4I_{11/2}$), from which it nonradiatively (NR) decays to the metastable state ($^4I_{13/2}$). The decay time τ_{21} (about 10 ms) is much longer than τ_{32} [in the order of nanoseconds (ns)]. Therefore, N_3 is approximately equal to zero, and an EDF can be described as a two-level system[4]. If the separation between Er^{3+} is decreased due to an increased number of dopant ions, they tend to form cluster. Due to clustering, ion–ion interaction increases and the metastable-state population decreases and degrades the EDFA performance. The cooperative upconversion (see Fig. 1) starts from the $^4I_{13/2}$ state, where excited-state ions exchange energy with each other. After transferring energy, a donor ion comes back to the $^4I_{15/2}$ state, an acceptor ion is excited to the $^4I_{9/2}$ state, and then NR decays back to $^4I_{13/2}$. By this process, metastable state $^4I_{13/2}$ population is reduced. If we assume that the signal and pump intensity distributions are separable in the

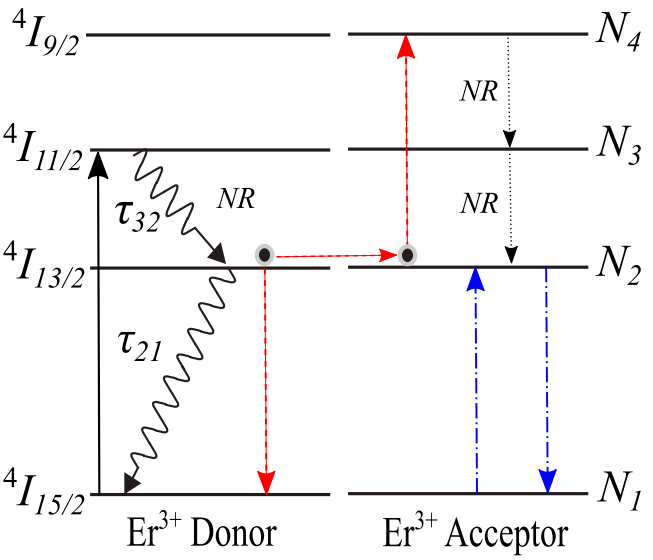

Fig. 1. Energy-level diagram of Er^{3+} ion[16]. Pump signal absorption and cooperative upconversion are indicated by black solid arrows and red dashed arrows, repectively. Stimulated absorption and emission at the signal wavelength are shown by blue dashed arrows.

EDF, the signal intensity (I_s) and the pump intensity (I_p) can be written by the following equations:

$$I_p(r,\Phi,z) = f_p(r,\Phi)I_p(z), \tag{1}$$

$$I_s(r,\Phi,z) = f_s(r,\Phi)I_s(z), \tag{2}$$

where f_s and f_p denote the signal and pump transverse intensity profiles, respectively. They are normalized in such a way that

$$\int_0^{2\pi} \mathrm{d}\Phi \int_0^{\infty} f_{p,s}(r,\Phi) r\,\mathrm{d}r = 1. \tag{3}$$

Similarly, the population density can be given as

$$N_i(r,\Phi,z) = g(r,\Phi)N_i(z), \tag{4}$$

where $g(r,\Phi)$ represents the normalized doping intensity profile. For a uniform distribution of erbium ions in the fiber core, $N_i(z)$ is equal to N_0, where N_0 represents the total erbium ion dopant concentration. The overlapping integral factor Γ_i between the fields and the dopant can be given as

$$\Gamma_{p,s} = \int_0^{2\pi} \mathrm{d}\Phi \int_0^{a} f_{p,s}(r,\Phi) g(r,\Phi) r\,\mathrm{d}r, \tag{5}$$

where a denotes the erbium ions' doping radius.

If we denote the fiber propagation direction as the z axis, the rate equations in the cylindrical coordinate system can be written as

$$\frac{\mathrm{d}N_2(r,\Phi,z,t)}{\mathrm{d}t} = \frac{\sigma_{\mathrm{ap}} I_p(r,\Phi,z)}{h\nu_p} N_1(r,\Phi,z,t) + \frac{\sigma_{\mathrm{as}} I_s(r,\Phi,z)}{h\nu_s} N_1(r,\Phi,z,t) - \frac{\sigma_{\mathrm{es}} I_s(r,\Phi,z)}{h\nu_s} N_2(r,\Phi,z,t) - A_{21} N_2(r,\Phi,z,t), \quad (6)$$

$$N_1(r,\Phi,z,t) + N_2(r,\Phi,z,t) = N_0(r,\Phi,z,t). \quad (7)$$

Here, N_1 and N_2 represent the ground-state and metastable-state-level populations, respectively; ν_p and ν_s denote the frequencies of the pump and the signal, respectively; h is a Planck constant; σ_{as} and σ_{es} are the stimulated absorption and emission cross-sections, respectively; σ_{as} is the absorption cross-section; and A_{21} is the spontaneous emission rate.

For the copropagating scheme, the signal and pump propagation equations can be written as

$$\frac{\mathrm{d}I_p(r,\Phi,z)}{\mathrm{d}z} = -\sigma_{\mathrm{ap}} N_1(r,\Phi,z,t) I_p(r,\Phi,z), \quad (8)$$

$$\frac{\mathrm{d}I_s(r,\Phi,z)}{\mathrm{d}z} = [\sigma_{\mathrm{es}} N_2(r,\Phi,z,t) - \sigma_{\mathrm{as}} N_1(r,\Phi,z,t)] \times [I_s(r,\Phi,z)]. \quad (9)$$

In Eqs. (8) and (9), the fiber loss has been neglected. From Eq. (9), the amplification condition can be expressed as[17]

$$\frac{N_2(r,\Phi,z,t)}{N_1(r,\Phi,z,t)} > \frac{\sigma_{\mathrm{as}}}{\sigma_{\mathrm{es}}}. \quad (10)$$

For amplification, the pump intensity must be greater than the threshold intensity I_{th}, which can be deduced from Eq. (10)[18]:

$$I_{\mathrm{th}} = \frac{\sigma_{\mathrm{as}} h\nu_p}{\sigma_{\mathrm{es}}\sigma_{\mathrm{ap}}\tau_{21}}. \quad (11)$$

Figure 2 shows the two sub-regions: the absorption and the amplifying regions of an EDF, which are determined by comparison with the threshold intensity. In the amplifying region, the pump intensity is greater than the threshold intensity. However, the condition is the opposite for the absorbing region. To explain these two different regions, the pump envelope in the fiber core needs to be analyzed. The optical pump signal propagates in the z direction through the fiber core as a fundamental linearly polarized (LP_{01}) mode. The intensity distribution of this fundamental mode in a step-index fiber can be given by $P_p(z)\psi_{01}(\lambda_p, r)$, where P_p and ψ_{01} represent the pump power and the envelope of the LP_{01} mode. The envelope of this mode is almost Gaussian and is given by[19]

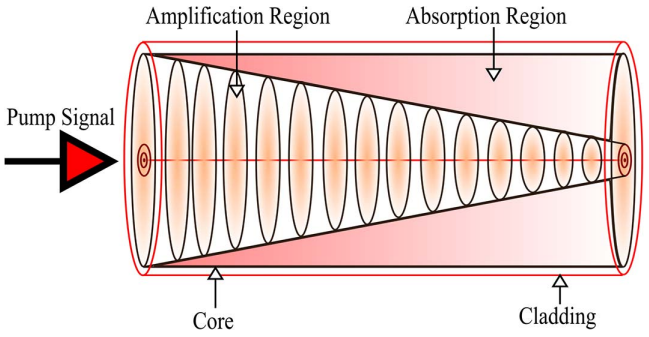

Fig. 2. Absorption and amplification region creation in an EDF.

$$\psi_{01}(\lambda_p, r) = \begin{cases} J_0^2\left(\frac{u_p r}{a}\right), & \text{for } r \le a \\ \frac{J_0^2(u_p)}{K_0^2(w_p)} K_0^2\left(\frac{w_p r}{a}\right), & \text{for } r > a \end{cases}, \quad (12)$$

where J_0 and K_0 denote Bessel and modified Bessel functions, respectively; u_p and w_p are the transverse propagation constants of the LP_{01} mode; a is the core radius of the step-index fiber.

If a uniform pump intensity could be maintained in the EDF core, the pump intensity would have gone below the threshold value for a specific EDF length. However, the pump signal propagates through the EDF core as a fundamental LP_{01} mode and has a nearly Gaussian shape. Due to the Gaussian nature of the pump signal, the signal intensity in the center of the core is the highest, and it gradually decreases towards the core–cladding boundary region. As the pump power near the core–cladding boundary region is smaller than in the center region, the absorption region gradually increases with pump signal propagation along the z direction. The pump signal intensity in the core–cladding boundary region might go below the threshold due to the tailing edge of the Gaussian intensity distribution, but at the same time it might remain above the threshold near the center of the core region, being the highest intensity portion of the pump signal. Due to this phenomenon, the absorption and amplifying regions gradually increase and decrease with the pump signal propagation along the z direction, respectively, as shown in Fig. 2.

In this Letter, the EDFA gain performance has been simulated by varying the doping radius and NA of the fiber with various pump powers. A typical forward pump EDFA configuration (as shown in Fig. 3) is modeled via OptiSystem (version 13), which allows for the design and simulation of optical fiber amplifiers. This simulation tool solves the rate equations to calculate the spatial distributions of optical power. Emission and absorption cross-section parameters, which are host dependent and specific for each doped fiber, of an EDF are already included in the software. The user can change the other important parameters, such as pump wavelength, signal wavelength, fiber length, core radius, and doping concentration, to evaluate the fiber amplifier performance. This software can also include the upconversion process in the simulation, provided that suitable parameters are chosen by

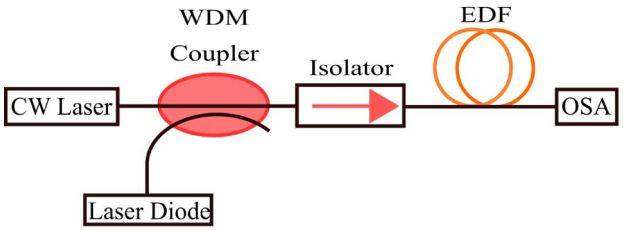

Fig. 3. A typical forward pump EDFA.

the designer[20]. In the simulation model, we have used 20 m of C band EDF with typical EDFA gain spectrum. The NA and core radius of the EDF are chosen as 0.32 and 1.8 μm, respectively. These parameters ensure the single mode operation of an EDF, which is essential to obtain high beam quality output at the signal wavelength. The EDF is used as the active gain medium for the EDFA and is pumped with a laser diode emitting at 980 nm. For the pump source, we have also chosen a laser diode, which can produce high beam quality output to ensure maximum excitation of the fundamental mode of an EDF. Other simulation parameters, such as metastable lifetime and saturation parameters, are chosen from Ref. [18]. The pump power emitting at 980 nm (from a laser diode) and signal power emitting at 1550 nm (from a continuous wave laser denoted as the CW laser) are coupled into an EDF via an ideal WDM. Three different pump powers, 20, 25, and 30 mW, and −20 dBm signal power are used to measure the EDFA performance. An isolator is used to reduce the back-reflection. In the simulation, the doping radius of the EDF is varied and EDFA performance is evaluated to determine the optimum doping radius of an EDF, which ensures the best EDFA performance. For determining the doping radius effect on the EDFA performance, we have divided the core into 100 concentric circular rings centered at the fiber core with various radii and deposited 1.04×10^{12} ions/m into an EDF. This number corresponds to 700 ppm (1000 ppm $= 1.84 \times 10^{25}\,\mathrm{m}^{-3}$) for a 1.6 μm core radius. Later on, we gradually reduced the doping radius, keeping the same number of dopant ions/m of EDF, and recorded the EDFA gain data for post processing. Finally, we processed that data using MATLAB to obtain the EDFA gain as a function of the doping radius. To include the upconversion process in the simulation, we have chosen both homogenous and inhomogeneous upconversion. For inhomogeneous upconversion, we have considered 2% relative ion percentage and 2 ions/cluster.

The EDFA gain curve, as shown in Fig. 4, is obtained by varying the doping radius of the erbium ion. The EDFA gain performance is analyzed by using three different pump powers (20, 25, and 30 mW). The EDFA gain varies with the doping radius. However, there is an optimal doping radius for which the gain is a maximum. For our simulation data, the optimal doping radius is 0.8 μm, which is not fixed for every EDF. If the EDF parameters (as mentioned in the previous section) are

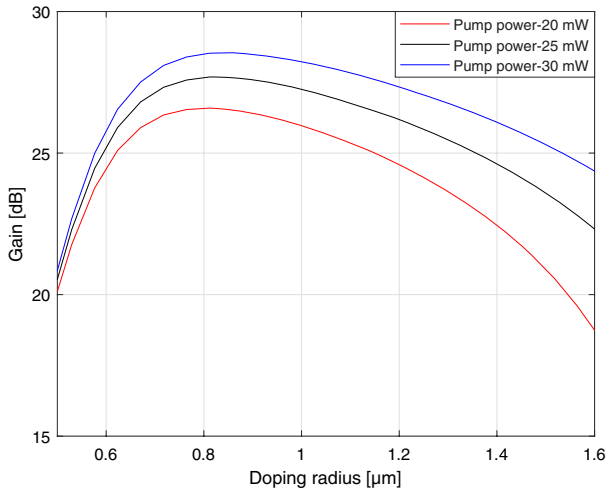

Fig. 4. EDFA gain with various doping radii.

changed, the optimum doping radius will also vary. The gain decreases whenever the doping radius increases or decreases from the optimal point. This phenomenon can be explained by using Fig. 2, where the amplifying and absorbing region creation in an EDF is discussed. If the doping radius is increased from the optimal point, the ions residing in the core–cladding boundary region will create an absorption region and decrease the EDFA gain performance. This phenomenon can be further explained by using various pump powers. As the pump power increases, the absorbing region decreases, which increases the EDFA gain performance. On the other hand, if the doping radius decreases from the optimal point, the same number of dopant ions needs to be used in a comparatively small volume. Therefore, the ion–ion separation decreases, which introduces detrimental clustering effects and reduces the EDFA performance (readers who are interested in detrimental ion–ion interaction effects on EDFAs and EDFLs are directed to read our recent publications[14,15]).

For comparison purposes, we have used three different doping radii (0.6, 0.8, and 1.0 μm) and measured the EDFA gain performance. For the specific EDF parameters used in the simulation, the best gain spectrum (maintaining maximum gain over 80% of the total band) is obtained for the optimal doping radius, as shown in Fig. 5. As the doping radius is increased or decreased from the optimal doping radius, the gain performance decreases. If the doping radius is increased from the optimal point, the gain performance decreases due to the increasing absorption region created by the dopant ions residing in the core–cladding boundary region. On the other hand, the gain performance decreases due to ion–ion interaction effects if the doping radius decreases from the optimal point. In this case, ions of the same number are concentrated in a smaller volume, and consequently, the dopant ions come closer and form clusters in the EDF, which is detrimental for EDFA performance. Due to the clustering effect, excited-state erbium ions transfer energy with each other and reduce the excited-state population, subsequently degrading the EDFA performance.

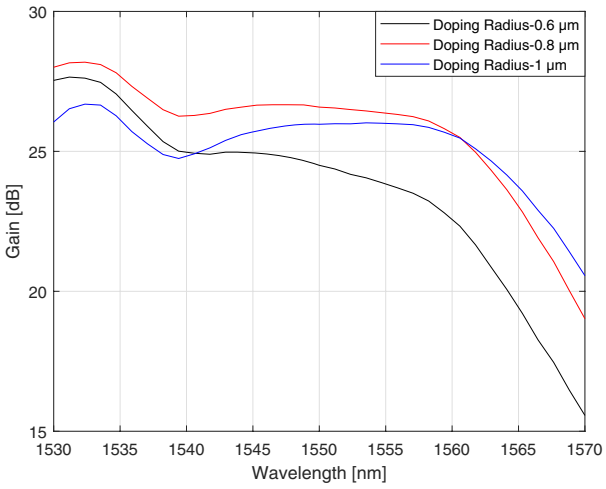

Fig. 5. EDFA gain spectra with various doping radii.

To achieve higher gain from the EDFA, more population inversion is required. This can be achieved by increasing the pumping intensity inside the fiber core. A higher NA is advantageous to increase the light coupling efficiency in the fiber core. Therefore, increasing the NA couples more light inside the fiber core and increases the gain performance, as shown in Fig. 6. This simulation has been done for three different pumping powers (20, 25, and 30 mW). As the pump power increases, more power is coupled into the fiber, which increases the population inversion in the active medium and improves the EDFA gain performance. But, the NA of a single mode fiber is determined by the operating wavelength and cannot be increased indefinitely. Alternatively, improved gain performance for an EDFA can be obtained by increasing the pump–dopant interaction. The optimal dopant ions distribution around the center of the core and the excitation of the fundamental mode of fiber ensure the maximum pump–dopant interactions. This happens due to the characteristics of the fundamental mode, which has a Gaussian shape. For this Gaussian shape, the pump intensity is highest in the core center and gradually decreases with radial distance. Hence, dopant ions distribution with an increasing doping radius gradually place dopant ions in the core–cladding boundary region, where they interact with gradually lower pump intensity. On the other hand, decreasing the doping radius increases the detrimental clustering effects, which reduce the excited-state population. If the dopant ions are distributed with an optimal doping radius, the pump–dopant interaction increases with reasonable clustering effects. Therefore, an optimal doping radius will help to efficiently utilize pump energy, which will subsequently increase the pump photon conversion efficiency.

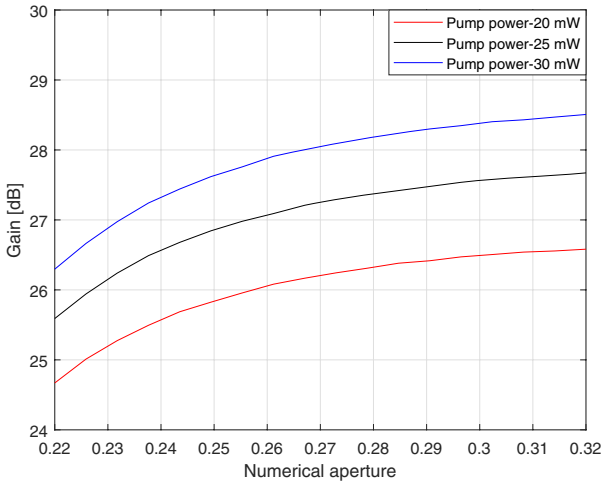

Fig. 6. EDFA gain performance as a function of NA with various pump powers.

EDFA is suitable for a wide range of applications in modern fiber optic communication systems. One of the main goals of the EDFA design is to obtain the maximum gain using a lower level of pump power. A maximum pump–photon conversion efficiency can ensure this desired goal. In this Letter, we have simulated the effects of the doping radius on the gain performance of an EDFA. It is found that the optimum doping radius in the EDF can increase the pump–photon conversion efficiency and consequently increase the gain performance of an EDFA. Deviation from the optimum doping radius of an EDF will degrade the EDFA performance. For observing pump intensity effects, EDFA gain performance is simulated for various NAs. It is well-known that a larger NA will increase the EDFA gain by increasing the pump intensity inside the core of the doped fiber. However, the NA of a single mode fiber is restrictive and cannot be increased indefinitely. Therefore, an alternative approach of using an optimal doping radius in an EDFA increases the pump–dopant interaction and increases the EDFA performance.

The authors acknowledge the support from King Fahd University of Petroleum and Minerals (KFUPM), King Abdulaziz City for Science and Technology (KACST) via KACST-TIC in Solid State Lighting (Nos. EE2381 and KACST TIC R2-FP-008).

References

1. G. P. Agrawal, *Fiber-optic Communication Systems*, 3rd Ed. (Wiley, 2002).
2. R. J. Mears, L. Reekie, I. M. Jauncey, and D. N. Payne, in *Optical Fiber Communication* (Optical Society of America, 1987), paper WI2.
3. B. Pedersen, A. Bjarklev, J. H. Povlsen, K. Dybdal, and C. C. Larsen, J. Lightwave Technol. **9**, 1105 (1991).
4. G. G. Du and G. F. Chen, Sci. China Series A: Math. **42**, 286 (1999).
5. F. Diana, B. Mahad, A. Sahmah, and B. M. Supaat, Faculty Electr. Eng. Univ. Teknol. Malaysia **11**, 34 (2009).
6. O. Mahran, M. S. Helmi, G. D. Roston, N. E. Sayed, and E. M. Gerges, Res. J. Appl. Sci. Eng. Technol. **7**, 3164 (2014).
7. R. I. Laming, D. N. Payne, and M. Tachibana, in *Optical Fiber Communication* (Optical Society of America, 1991), paper ThM3.
8. M. N. Zervas, R. I. Laming, and D. N. Payne, in *IEE Colloquium on Optical Amplifiers for Communications* (1992), p. 7/1.
9. J. R. Armitage, Appl. Opt. **27**, 4831 (1988).

10. B. J. Ainslie, J. R. Armitage, S. P. Craig, and B. Wakefield, in *1988 Fourteenth European Conference on Optical Communication, ECOC 88* (1988), p. 62.
11. M. Ohashi, J. Lightwave Technol. **9**, 1099 (1991).
12. P. Myslinski, D. Nguyen, and J. Chrostowski, J. Lightwave Technol. **15**, 112 (1997).
13. H. Masuda, A. Takada, and K. Aida, J. Lightwave Technol. **10**, 1789 (1992).
14. M. Z. Amin and K. K. Qureshi, in *2015 IEEE 28th Canadian Conference on Electrical and Computer Engineering (CCECE)* (2015), p. 1383.
15. M. Z. Amin and K. K. Qureshi, Chin. Opt. Lett. **15**, 010601 (2017).
16. B. C. Hwang, S. Jiang, T. Luo, J. Watson, G. Sorbello, and N. Peyghambarian, J. Opt. Soc. Am. B **17**, 833 (2000).
17. A. Hassani, E. Arzi, and F. E. Seraji, Opt. Quantum Electron. **39**, 35 (2007).
18. C. R. Giles and E. Desurvire, J. Lightwave Technol. **9**, 271 (1991).
19. A. W. Snyder and J. D. Love, *Optical Waveguide Theory* (Chapman and Hall, 1983).
20. https://optiwave.com/category/optisystem-manuals/optisystem-tutorials/.